Neurotherapeutics (2017) 14:107–118
DOI 10.1007/s13311-016-0491-x

REVIEW

Electrical Impedance Myography and Its Applications in Neuromuscular Disorders

Benjamin Sanchez[1] · **Seward B. Rutkove**[1]

Published online: 3 November 2016

Abstract Electrical impedance myography (EIM) refers to the specific application of electrical bioimpedance techniques for the assessment of neuromuscular disorders. In EIM, a weak, high-frequency electrical current is applied to a muscle or muscle group of interest and the resulting voltages measured. Among its advantages, the technique can be used noninvasively across a variety of disorders and requires limited subject cooperation and evaluator training to obtain accurate and repeatable data. Studies in both animals and human subjects support its potential utility as a primary diagnostic tool, as well as a biomarker for clinical trial or individual patient use. This review begins by providing an overview of the current state and technological advances in electrical impedance myography and its specific application to the study of muscle. We then provide a summary of the clinical and preclinical applications of EIM for neuromuscular conditions, and conclude with an evaluation of ongoing research efforts and future developments.

Key Words Electrical impedance · muscle · myopathy · neurogenic disease · disuse · injury

Introduction

The concept of using localized surface electrical impedance measurements as a method for the evaluation of neuromuscular disease was introduced in 2002 [1]. The term "electrical impedance myography" (EIM) was then suggested the following year to help establish the method as an independent, impedance-based approach for the assessment of conditions affecting muscle and nerve [2]. Since then, EIM has been applied to a variety of clinical conditions ranging from disuse atrophy [3] to amyotrophic lateral sclerosis (ALS) [4], both as a primary diagnostic technique and as a biomarker to assess disease progression and response to therapy. Recent technological innovations have also led to new devices for rapid data acquisition in the clinic and laboratory [5]. In a quest to help develop a detailed understanding of the data and to facilitate improvements in the technique, applications to a variety of animal models of disease have also been pursued [6–9], as well as computer-based modeling [10].

In this review, we provide a brief overview of the history of impedance techniques in medicine, the underlying theory associated with the measurement and analysis of impedance, a review of its clinical and preclinical uses in neuromuscular disease, and, finally, a discussion of ongoing developments and planned innovations. While we try to make clear that EIM remains in a state of refinement, we hope that the reader will come away with a deeper appreciation for the technique's strengths, limitations, and future potential.

History of Muscle Electrical Impedance and Current State of the Art

Whereas throughout the twentieth century most of the medical and physiological communities were mainly interested in the inherent electrical potentials produced by muscle and nerve, by the 1960s other investigators began to evaluate for the first time the impedance properties of muscle. For example, the static impedance properties of muscle were evaluated in single muscle fibers [11], including their spatial dependence [12, 13], as well as broader studies on excised muscle [14–16]. In parallel with these initial muscle-specific studies, the use of electrical

✉ Seward B. Rutkove
srutkove@bidmc.harvard.edu

[1] Department of Neurology, Division of Neuromuscular Disease, Beth Israel Deaconess Medical Center, Harvard Medical School, Boston, MA 02215, USA

impedance found other noninvasive medical uses, perhaps the most well known being electrical impedance cardiography [17, 18], which measures blood impedance changes to determine cardiodynamic parameters, and bioelectrical impedance analysis [19, 20] for estimating body composition. By the early 2000s, impedance innovations were being applied to other body regions, including skin [21] and breast [22], as well as approaches for imaging with impedance termed electrical impedance tomography [23]. In 2002, impedance methods were applied for the first time for the evaluation of neuromuscular disease [1].

Electrical Impedance Myography

Basic Measurement Principles

EIM is usually performed using 4 electrodes to minimize electrode polarization, thus maintaining signal quality [24, 25]. Figure 1 shows an example of 4 electrodes placed on the skin. The outer electrodes apply and measure an alternating sine-wave current stimulus in the kHz to MHz frequency range. As a result of the current applied, the tissues generate a response in the form of an alternating voltage signal that is sensed by the inner electrodes. The ratio and normalization of the voltage and current amplitudes and phase delays provides a simple approach to measuring the impedance magnitude $|Z|$ and phase angle θ at any particular frequency. Below, we provide an overview of the current state of art and technological opportunities that can be brought into EIM.

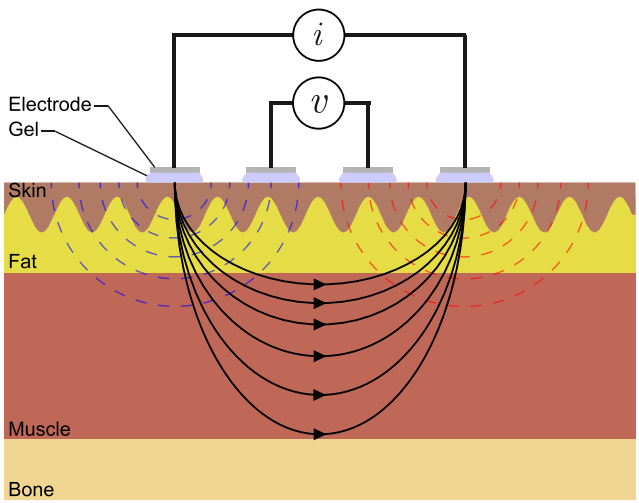

Fig. 1 Schematic representing the measurement of electrical impedance using 4 surface gel-adhesive electrodes placed over the skin. The flow of electrical current through tissues between the outer electrodes generates a potential that is measured by the inner electrodes

Electrode Materials

There are a variety of electrode materials available for recording bioelectrical potentials in other applications, such as nerve conduction studies and electromyography, that can be used for EIM [26–28]. The most common is the silver/silver chloride electrode, which is available in both reusable and nonreusable forms. Dry electrodes (e.g,. metal-plate electrodes) are another alternative [29, 30], which offer the advantage of not causing inadvertent contact between adjacent electrodes secondary to gel escaping from beneath the electrodes. Further, the low cost and short distances achievable between metal electrodes using standard printed circuit technology makes them an attractive solution when measuring small muscles, for example in animal models. Another material to be used in EIM are textile dry electrodes, which can be integrated into garments incorporating wearable electronics and could be used for long-term EIM monitoring during daily activities; however, these may suffer from inferior skin-electrode impedance, noise interference, and motion artifacts [31]. Recent advances in micro- and nanotechnologies offer new electrode alternatives, for example using microneedle electrode arrays [32].

Electrode Positioning

The first EIM experiments had placed the current electrodes on the dorsum of both hands for measuring biceps and on the dorsum of both feet for measuring tibialis anterior and quadriceps [33]. This electrode configuration had the advantage of large spatial resolution and a reduction in the contribution of subcutaneous fat to the acquired impedance values; however, it had the disadvantages of being inconvenient to apply, being less muscle-specific, and that alterations in joint position could drastically alter the outcomes. The alternative approach, which has since become the standard method, is to perform localized EIM measurements with all 4 electrodes linearly arranged over a muscle of interest. However, the sensitivity of such measurements to detect disease severity and progression depends on the specific electrode arrangement used [34], and will be affected by surrounding tissues, including skin, subcutaneous fat, and bone [35].

EIM Measuring Devices

Instruments to measure impedance may be most simply categorized by their functional principles. Early in the last century, the common method used to measure impedance was the Wheatstone bridge circuit [36–38]. Today, there are more sophisticated measurement concepts available [39–48]. Ultimately, the choice of the right instrumentation will depend on many factors,

including accuracy, ease of use, cost, and measurement range. In all, there will be different sources of error that may affect the impedance and the reproducibility of results, including parasitic capacitances between cables [49–53], inconsistent electrode contact [54], electrode positioning errors [55–58], or a combination of factors [59].

Electrical Impedance Myography Data Representation

The impedance, Z, measures the obstruction to the flow of electric current through tissues and is defined by 2 components, with the standard notation

$$Z = R + jX,$$

where R and X are the resistance and reactance parts of the impedance distinguished by the unit j to avoid confusion with the sum/addition operation between values.

When the reactance is represented against the resistance (Fig. 2), the length of the impedance vector is the magnitude of the impedance $|Z|$ connecting the ending point (R, X) to the origin of coordinates. The impedance phase angle θ then describes the angle formed by *the impedance vector*. The relationship between the magnitude and phase value of the impedance and its resistance and reactance parts is

$$|Z| = \sqrt{R^2 + X^2} \text{ and } \theta = \tan^{-1}\frac{X}{R},$$

or, equivalently,

$$R = |Z|\cos\theta \text{ and } X = |Z|\sin\theta.$$

As the frequency is varied, the impedance defines characteristic plots that are related to the underlying structure and properties of muscle. Sweeping through a frequency range of interest allows one to obtain a complete impedance characterization of the muscle being tested. In muscle measured between the kHz and MHz range, the reactive component of

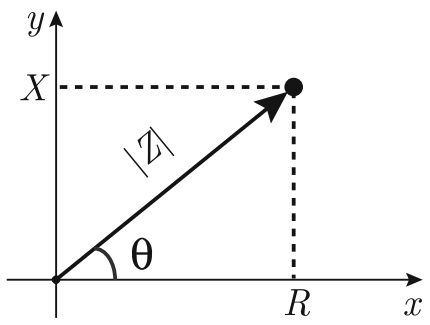

Fig. 2 Representation of a temporally-stable impedance Z in Cartesian and polar coordinates. The resistance R and reactance X and, equivalently, the magnitude $|Z|$ and phase θ, are the components that describe the impedance uniquely in both coordinate systems

cells is caused mainly by the myofiber membrane, which behaves as an electrical insulator Also, owing to the dispersive nature of biological samples, the representation of multifrequency impedance data describes a depressed semicircular arc, the nature of which is further discussed below.

EIM Data Modeling and Analysis

To establish a relationship between EIM and myofiber morphology and physiology, the use of theory and simulations are required to obtain a biophysical model or, equivalently, an electrical circuit model able to explain EIM data. Based on experimental observations, the impedance frequency dependence can be modeled empirically [60, 61], using the model proposed by Cole [62]. The Cole model summarizes the frequency dependence of EIM into 4 parameters that have a direct interpretation in terms of the geometrical and electrical properties of skeletal muscle fibers (Fig. 3). The highest resistance value in the x-axis of the Cole plot R_0 is the resistance at zero frequency (i.e., as if it were possible to measure with a constant current of 0 Hz); this resistance is associated with extracellular compartment, R_e. The lowest resistance value in the x-axis of the Cole plot is the resistance at infinity frequency R_∞ (i.e., as if it were possible to measure with an alternating current of infinite frequency), a result of the parallel combination between the resistances of the intracellular and extracellular compartments:

$$\frac{1}{R_\infty} = \frac{1}{R_e} + \frac{1}{R_i}.$$

How depressed the center of the arc is with respect to the x-axis is described by the α parameter, a factor that accounts for the variation in cell size. The range of values of α is from 0 to 1, the latter indicating perfectly homogenously sized, spherical cells. The apex of the impedance arc (i.e., maximum of reactance) corresponds to the characteristic frequency, f_c, at which the current is evenly divided between the intracellular and extracellular compartments [63].

Another aspect of muscle impedance characteristics is its anisotropy, or directional dependence: current flows more easily along muscle fibers than across them. Thus, *in vivo* impedance measurements of skeletal muscle can be used to estimate an empirical anisotropic ratio of skeletal muscle dielectric properties (i.e., those material properties describing the tissue's chargeability) in longitudinal and transverse directions relative to the major muscle fiber direction [15, 64, 65]. Measurement of surface anisotropy is also possible, although limb size and subcutaneous fat will substantially affect the anisotropic values obtained [66].

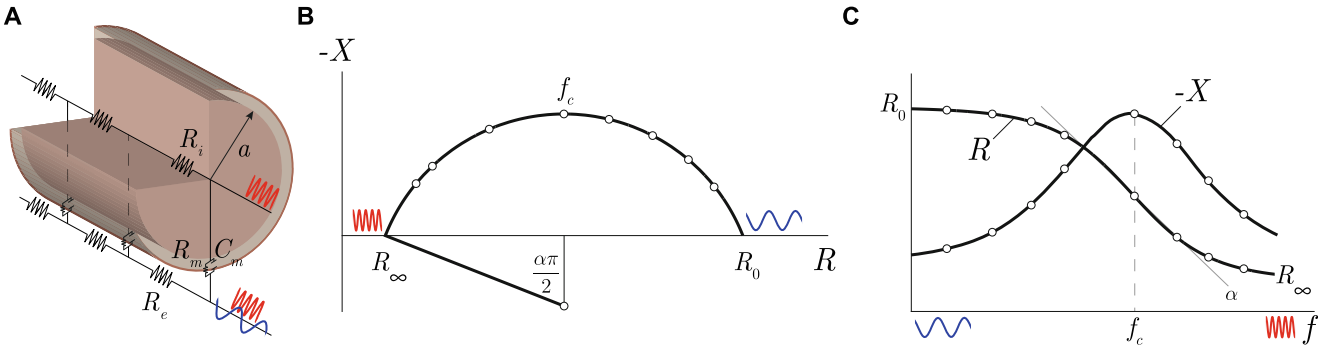

Fig. 3 (A) Schematic representation of the equivalent electrical circuit of a cylinder shaped myofiber with radius a. The circuit parameters model the extracellular resistance R_e, intracellular resistance R_i, membrane surface capacitance C_m, and membrane resistance R_m. Owing to the membrane permeability at low frequencies (illustrated by the blue sine-waves), only high-frequency current (illustrated by the red sine-waves) can flow through the intracellular compartment. (B) Representation of the Cole impedance model in the complex plane and, equivalently, (C) the resistance and reactance as function of the frequency (C)

Disease-Specific Applications

EIM has been applied to a variety of neuromuscular conditions. As the purpose of this review is to focus on applications of impedance in the assessment of neuromuscular disease, we will not offer specific detailed comparisons as to the advantages and disadvantages of the technology *versus* other widely accepted approaches of muscle assessment. An important consideration, however, is that the major value of EIM has been in the evaluation of disease severity, progression over time, and response to therapy, and not in assisting in establishing an initial diagnosis. While such diagnostic categorization may be feasible using EIM [67, 68], the main focus of this review will be in showing its potential uses in specific disorders as a means of assessing disease severity, progression, and response to therapy.

One of the ongoing challenges with EIM is the identification of which of the multitude of potential parameters is most effective in which condition. While much of the initial work focused on the 50 kHz phase values [1, 3, 69, 70], over the last several years other parameters have been used, including single-frequency reactance and resistance values [71], as well as multifrequency measures [72–76]. Assessing the muscle's anisotropic properties also may be of value [67, 77]. Most recently some of the Cole parameters described above have also been evaluated [78]. As different neuromuscular disorders are associated with different muscle pathologies, it should be anticipated that different EIM parameters may be more useful in some conditions than in others. Moreover, depending on the mechanism of a specific disease, the EIM parameters that are most sensitive to the drug effect could also differ. Thus, which specific EIM parameter is most effective in a given condition remains an open question that will likely only be resolved with additional study and experience. Nevertheless, in this review, we also provide information on that aspect of EIM application.

Neurogenic Disorders

Given the marked muscle fiber and global muscle atrophy produced by primary neurogenic disorders, it is perhaps not surprising that impedance methods are sensitive to the changes induced by motor neuron loss or injury. Both progressive diseases and nerve trauma have been studied.

Amyotrophic Lateral Sclerosis

The use of EIM for tracking ALS progression was first reported in 2002 [1], when progressive reduction in 50 kHz EIM phase values were observed in the quadriceps of a man diagnosed with ALS who had clinical weakness only affecting the upper extremities. Two subsequent studies confirmed the sensitivity of the technique and the 50 kHz phase to disease progression in patients with ALS [4, 79]. The second of these, a multicenter study, showed that EIM had the potential for reducing the size of a clinical trial by more than 50 % compared with standard clinical outcomes [4]. A major strength of EIM for the evaluation of ALS progression is its ability to be used flexibly in the body region undergoing deterioration at the time of study. Thus, multiple limbs can be easily assessed, but only those that are deteriorating most rapidly at the time of the study can be utilized in the analysis. Such an approach may offer the possibility of substantially reducing sample size in clinical trials as the data can be enriched with the most symptomatic body region [4].

Another possible strength of EIM is its potential value in assessing bulbar dysfunction. This is especially important as there are few easily quantifiable assessment tools available. Recent studies have shown EIM's ability to discriminate ALS-affected tongue from healthy tongue using a simple 4-electrode array constructed on a tongue depressor or similar base [80, 81], using both single and multifrequency phase data. Further, a computer modeling study has shown that changes in impedance with tongue atrophy likely reflect

tongue properties and are not simply an effect of decreasing tongue volume with disease progression [82].

In addition to these direct clinical applications, EIM has been studied in ALS SOD1 G93A mouse and rat models [74, 83]. These animal investigations have confirmed EIM's ability to track disease progression, as well as its strong relationship to standard electrophysiologic and functional measures of disease status, including the compound motor unit action potential (CMAP) amplitude, the motor unit number estimate (MUNE) [84], and force [78]. The phase at 50 kHz, as well as a variety of multifrequency impedance parameters, have been shown to be useful in this regard [74]. Ultimately, changes in the inherent dielectric properties of muscle are at least partially responsible for such impedance changes, including increased conductivity across, but not along, the myofibers compared with wild-type animals [68].

Spinal Muscular Atrophy

Studies have identified that EIM values, including single and multifrequency phase, resistance, and reactance values correlate to disease severity in milder forms of spinal muscular atrophy (SMA) (types 2 and 3) [75]. It also shows a difference longitudinally over time compared with healthy children in whom the latter demonstrate a gradual increase in values (e.g., increasing phase values at 50 kHz in specific muscles), likely due to myofiber growth and maturation [76]. A recent multicenter study has shown that it is possible to distinguish infants with type 1 SMA from healthy children [85], and to detect EIM differences over time between these two groups of very young children. Parallel animal work has shown that EIM 50 kHz phase values can capture the effect of early treatment with antisense oligonucleotides in the SMAΔ7 mouse model [86], comparable with CMAP and MUNE [9]. Given the remarkable progress made in the broader field of SMA therapeutics, EIM may find value in monitoring and testing a variety of new therapies as they become available in children and adults.

Nerve Injury and Radiculopathy

Given the technique's sensitivity to disease progression in ALS, EIM might be anticipated to be sensitive to other disorders characterized primarily by axonal loss. Indeed, the EIM technique has proven useful in the diagnosis of radiculopathy, with specificity and sensitivity similar to that of needle electromyography (EMG) [87, 88]. Unlike needle EMG, however, there is no dichotomous outcome (e.g., presence *vs* absence of fibrillation potentials). For this reason and also because there is a fairly wide range of normal values, in order to employ EIM for this purpose, it is necessary to compare measures on the affected side to those on the unaffected side [88]. For example, relative reductions in EIM 50 kHz phase values in biceps and deltoid on the affected side compared with the unaffected side would be considered consistent with a C5 radiculopathy. This approach is similar to the way in which CMAP or sensory nerve action potential amplitudes are compared side by side when performing nerve-conduction studies.

Studies in rat models of sciatic injury have provided analogous findings to those of CMAP and MUNE [84], with marked reductions in 50 kHz phase values shortly after injury that gradually return to baseline values over time. Unlike CMAP and MUNE, however, which can both decrease to a value of zero (i.e., the complete absence of a response), EIM values show less dramatic alteration as the impedance of all living and nonliving tissues is greater than zero.

Other Neurogenic Disorders

Motor or sensorimotor axonal polyneuropathies, in which there is the muscle atrophy distally would be anticipated to produce substantial impedance alterations in foot and leg muscles. The use of EIM, however, in these conditions has, to our knowledge, not been studied, possibly because the evaluation of such conditions is generally considered a strength of standard electrophysiologic techniques. Nonetheless, it is possible that EIM could be useful as a biomarker for monitoring progression or assessing drug efficacy in slowly progressive polyneuropathies (e.g., Charcot-Marie-Tooth disease). Finally, although not neurogenic disease per se, to our knowledge, disorders of the neuromuscular junction, such as myasthenia gravis and Lambert–Eaton myasthenic syndrome, have also not been studied.

Myopathic Conditions

Unlike neurogenic disorders, myopathic disorders may show relatively limited atrophy, despite causing substantial weakness and disability. A major reason for this is that most chronic myopathies are accompanied by substantial compositional changes in the muscle—including the deposition of fat and connective tissue. In acute or subacute autoimmune conditions, there may also be edema and inflammation [89]. Moreover, myofiber size may vary considerably in all of these [90]. Regardless, these major structural and compositional changes would be expected to affect the dielectric properties of tissue, thus making EIM a very appropriate tool for evaluation of this group of disorders.

Duchenne Muscular Dystrophy

EIM 50 kHz phase has been shown to discriminate effectively healthy boys from boys with Duchenne muscular dystrophy (DMD) under 7 years of age [91]. More importantly, clinical studies have found EIM phase multifrequency parameters are sensitive to disease progression in older (>7 years) and to

some extent in younger (<7 years) boys (unpublished results). Given the technique's high reproducibility [5] and the fact that it requires minimal patient cooperation, it may offer a reliable and objective alternative to standard functional measures in DMD trials, such as the 6-min walk test. If that proves to be true, clinical studies could be completed with fewer boys in a shorter period of time than is currently possible. EIM also appears sensitive to the beneficial effect of steroids (unpublished data).

These human data have also been supported in studies in the muscular dystrophy (*mdx*) mouse, a standard mouse model of DMD. One study showed consistent and significant differences in 50 kHz phase reactance and resistance values between wild-type and *mdx* mice [8]. In this animal model, EIM values also correlated to muscle fiber size, the amount of connective tissue deposition [8], and also to T2 signal on magnetic resonance imaging (MRI) [92]. EIM has also shown sensitivity to the impact of myostatin inhibition in both wild-type and *mdx* mice [93].

Facioscapulohumeral Muscular Dystrophy

A study in patients with facioscapulohumeral muscular dystrophy revealed reductions in reactance values in specific muscles that correlated to the degree of abnormality on MRI [94]. Given the heterogeneous nature of this disorder, a tool such as EIM that can be applied flexibly at the bedside to quantify status of different muscle groups throughout the body could be especially useful as a biomarker in future therapeutic trials in this condition.

Myotonic Dystrophy

Myotonic dystrophy has been studied in mouse models only. Unpublished data suggest EIM may detect the presence of disease and the effect of therapeutic intervention. Its inclusion in future clinical trials in this condition is also being considered.

Inflammatory Myopathies

Marked reductions in the 50 kHz phase were identified in the quadriceps of individuals with inclusion body myositis, a muscle that is particularly affected in this disease [1]. A major contributor to this reduction in phase was through an increase in muscle resistivity, likely owing to replacement of normal healthy muscle tissue with fat. Another study found reductions in the 50 kHz phase in patients with inflammatory myopathies more broadly (inclusion-body myositis, as well as dermatomyositis and polymyositis) that correlated with clinical status [69]. Much of the work in these conditions was pursued early in the development of EIM technology and thus deserves to be revisited for more complete study and characterization using more advanced systems.

Critical Illness Myopathy

Another potential application of EIM is in the evaluation of patients with critical illness myopathy. Having a tool that can readily assess the development of this condition in patients in intensive care units would be very helpful. However, superimposed disuse effects (described below), without frank critical illness myopathy, may make it challenging to distinguish between the two. Moreover, it is not clear how critical illness myopathy characterized by primary muscle fiber inexcitability would impact the impedance signature. Nevertheless, given the technique's potential ease of application, its use for monitoring muscle status in this group also deserves further study.

Sarcopenia, Disuse, and Cachexia

The application of EIM to this group of disorders extends beyond the standard purview of standard electrodiagnostics, which would be expected to be normal or show only minimal change in recorded CMAPs and motor unit action potentials on needle electromyography [95]. In humans, this condition is mainly characterized by type 2 fiber atrophy [89]. In the case of longer-standing problems, such as sarcopenia, or muscle wasting with aging, there may also be a concomitant increase in connective tissue and to some extent fat in the muscle, thus affecting the composition of the tissue and accompanying impedance values.

Sarcopenia

Reductions in muscle impedance associated with sarcopenia were first detected on a cross-sectional study of 100 people [96]. A quadratic relationship between EIM 50 kHz phase in tibialis anterior and gastrocnemius was identified for both men and women, with a stronger relationship to age in the former. The reduction in these values with age was most pronounced in both sexes for people over 60 years of age. In addition, in that same study, 4 people over 75 years of age without any superimposed neuromuscular condition measured longitudinally demonstrated a decline over time.

A subsequent cross-sectional study found a decrease in the 50 kHz reactance rather than the 50 kHz phase was observed in older individuals. This was more marked in the lower extremities than the upper extremities (the latter not having been studied previously) and once again to a greater extent in men then women [71]. In fact, both this study and the earlier study were consistent with previous work showing that other markers of sarcopenia also showed greater reductions in men than women [97], and that the lower extremities usually

demonstrated more marked alterations than the upper [98]. The differences between the previously identified changes in phase and the changes in reactance have not been explained (although reactance was not evaluated in the earlier study).

Ongoing studies in sarcopenia have shown that, in older individuals, there is a significant relationship between EIM values in the lower extremities and function, including primary force production, as measured by the 1-repetition maximum using a leg press (unpublished data). Possible long-term applications of the EIM technique for this population of individuals may include monitoring exercise to forestall or reverse muscle decline, as well as to assess the effects of pharmacologic interventions. Ongoing animal studies may also help support the construct validity of these relationships by providing a histologic basis for some of these differences in aged muscle.

Disuse Atrophy

Muscle atrophy due to disuse was studied in a group of patients with ankle fractures who underwent measurement of their tibialis anterior muscles shortly after being nonweightbearing for 6 to 8 weeks [3]. Patients then underwent a single repeat measurement after they were fully weightbearing for several weeks. In all patients measured, the 50 kHz phase increased in tibialis anterior, with a mean increase of at 28.3 % (range 8.8–44.2 %), consistent with recovery.

Results from a study in rats undergoing hindlimb suspension were consistent with the findings seen in humans. During the study, the hindlimbs were removed from weightbearing for up to 2 weeks. To do so, the animals were placed in a specially designed cage such that the animals were suspended by their tails and were otherwise free to walk around the cage on the fore limbs, with full access to food and water [73]. After 2 weeks of suspension, multifrequency phase measures dropped by 33 %; after 2 weeks of being released from suspension, the animals had only partially recovered, still being, on average, 19.5 % lower than baseline. Another study evaluating a group of mice that were in microgravity for 12 days aboard the final Space Shuttle mission (STS-135) also showed substantial decrease in the same multifrequency phase measure—reaching values 43 % lower than a group of earth-bound animals [72].

Whereas studies in cachexia have, to our knowledge, not been investigated, given its similar pathology to disuse and sarcopenia, analogous alterations in muscle impedance measures are anticipated. The increasing interest and study of all of these types of conditions may make EIM a natural tool for their evaluation.

Traumatic Injury of Muscle

Traumatic injury to muscle, outside of related orthopedic trauma and consequent disuse, has been also studied in a group of male elite soccer players, three of whom were measured longitudinally after undergoing some form of injury [99, 100]. The injuries included hematoma due to direct trauma, a partial muscle tear, and a strain of various lower-extremity muscles. In all cases, the impedance values on the injured side decreased with injury and gradually recovered over time as the injury resolved, consistent with inflammation and hematoma formation.

Muscle injury induced by eccentric contractions to quadriceps has been studied in *mdx* and healthy mice. Significant reductions in phase values were observed over a period of 48 h (unpublished data). In particular, the characteristic frequency f_c increased in both wild-type and *mdx* mice, likely caused by a significant decrease of the surface membrane capacitance. A decrease in resistance caused by the presence of edema was confirmed with an increased T2-signal using MRI. These findings suggest EIM can detect changes caused by the disruption of the sarcolemma and t-tubule system in this animal model. Given the wide variety of types of muscle injury, additional study of this broad pathologic mechanism in animals, as well as in humans, is warranted.

Current and Future Directions

The application of EIM for the evaluation of nerve and muscle disorders involves a variety of challenges. In particular, further theoretical, engineering, and clinical work needs to be completed before EIM can be expected to reach its full potential. Moreover, the specific requirements for its successful implementation in each of these disorders also need to be better defined. Fortunately, in addition to all the work described above that has been completed, there is additional ongoing study and steady progress on a variety fronts that we highlight here.

Clinical Trials

First, there remain a number of efforts focused on the application of EIM to different specific conditions. For example, EIM is being incorporated into a number of ongoing clinical studies in ALS, SMA, DMD, facioscapulohumeral muscular dystrophy, and planned future trials in sarcopenia and potentially other muscular dystrophies. Some of these trials incorporate improved measurement approaches. For example, in one ongoing study in ALS [101], a smaller EIM probe is being used to evaluate hand muscles—a body region that is markedly affected by the disease but that has, to date, remained mostly unstudied. Another future study may seek to evaluate

the effects of therapy in young, presymptomatic children with DMD. This study may demand evaluation of other groups of muscles (e.g., gluteal muscles and iliopsoas) not previously assessed with the technology.

Relationship to Pathology

It would be valuable to establish more concrete relationships between EIM measures and muscle pathology. As noted earlier, impedance modeling can be used to reflect structural and compositional changes in muscle. For example, it is known the characteristic frequency depends on myofiber diameter. Thus, it may be possible to use it to infer an approximation of mean myofiber cross-sectional area [8]. In addition, the alpha parameter, α, also discussed earlier, may also provide insights in to the distribution of fibers around that mean. Similarly, evaluating impedance parameters at higher frequencies may provide insights into intracellular condition. For example, one study identified differences in high-frequency impedance parameters in type 1-predominant and type 2-predominant muscle in the rat, consistent with larger and increased number of mitochondria in type 1 fibers [102]. Thus, this work has the potential of providing novel measures of muscle status with specific pathologic implications otherwise only obtainable via muscle biopsy. Current animal research efforts are focused on evaluating EIM's relationship to cell size, mitochondrial characteristics, the degree of fibrosis and fatty infiltration in a muscle, the presence of glycogen storage abnormalities, and myofiber disorganization.

Computer Modeling

Further engineering work is necessary to identify the most effective electrode configurations to reduce the impact of subcutaneous fat, as well as ensuring effective depth of current penetration into muscle and capturing muscle's anisotropic qualities. Electrical impedance methods are highly dependent on the electrode size, spacing between electrodes, size of muscle, and thickness of skin and subcutaneous fat. As of today, most of the work has used simple linear electrode arrangements, the design of which has been based mainly on intuition [10]. Robust electrode configurations will be needed to exploit fully the value of EIM in the assessment of muscle condition across the disease and injury spectrum. Such modeling may also be useful for evaluating other technological advances, including micro- and nanoelectrode needle methodologies, discussed earlier [32].

Impedance During Contraction

The measurement of muscle impedance in real time during contraction actually represented some of the earliest applications of electrical impedance techniques specifically to muscle. For example, in 1912, McClendon [103] reported a 30 % decrease in impedance magnitude during isometric contraction with tetanic stimulation. Twenty years later, another study [104] reported reductions with both twitch and tetanic stimulation. In contrast, Bozler [105] and Bozler and Cole [106] found, *in vitro*, the impedance actually increased with isometric force in muscle. These opposing results were attributed to the experimental setup and changes in muscle shape occurring during contraction [105].

Over the last few decades, there have been additional efforts to evaluate impedance change during muscle contraction [1, 70, 107], and again some contradictions have been found. For example, Shiffman et al. [2] found consistent results with those observed by Bozler [105] in a healthy subject and a patient with polymyositis during voluntary isometric contractions. Others, in contrast, reported a decrease in the biceps brachii impedance after repeated isometric contractions [108]. Impedance has also been reported to decrease with muscle fatigue induced by prolonged nerve and muscle stimulation [109].

Differing results notwithstanding, the concept of using impedance to measure contractile properties in health and disease is attractive as it could offer new insights into the mechanics of muscle contraction, one area in which standard electrophysiologic techniques are relatively weak. In fact, current standard approaches such as needle EMG or nerve conduction studies only measure up to the point of muscle fiber depolarization, ignoring entirely the contractile process itself. Supporting this application, recent animal studies have shown impedance alterations in muscle contraction are disease-dependent [110]. Further development and application of impedance for the measurement of muscle contraction in real time could serve as a useful research tool with potential long-term clinical value.

Impedance Imaging

Electrical impedance imaging has been successfully applied to lungs [111], breast [112], prostate [113], and brain [114] in the form of electrical impedance tomography. In muscle, Silva [115] and Silva et al. [116] detected impedance changes by imaging the muscle during isometric maximum voluntary contraction and under repetitive contractions. Imaging muscle with impedance could provide unique insights into the spatial distribution of disease to assist in biopsy location (in muscle at rest) or as a novel approach to evaluating the intricacies of muscle contraction in 2 and 3 dimensions in real time.

Telehealth Monitoring

Modern-day electronics, the Internet of Things, and the ubiquitous smartphone, make other potential applications of EIM possible. In particular, the miniaturization of EIM measuring

systems into small handheld or implantable devices [117] will open a new clinical trial paradigm in which muscle condition can be tracked at home on a daily basis. Ultimately, frequent measurements by patients or caregivers at home could improve the ability to detect disease progression in ALS and other slowly progressive neuromuscular conditions. The hope is that the ability to detect disease progression more effectively will also make it possible to speed clinical therapeutic testing. Such an approach could also have application in other areas such as self-measurement after injury or during rehabilitation or to assess muscle condition as part of an exercise training program. Major advantages to this kind of approach include both increased convenience for the individual, as well as reduced costs to the society as a whole.

Conclusion

As evidenced by the number of recent or ongoing studies employing EIM, which are focused either on technological development or the procedure's direct application in the clinical arena, it is clear that the technique may have wide value in the assessment of neuromuscular disorders and muscle health more broadly. As the medical community learns the underlying principles of bioimpedance theory and familiarizes itself with the outcomes and specific applications of this technology, we believe that EIM will gradually be adopted into the standard repertoire of neuromuscular assessment tools.

Acknowledgments This work was supported by the National Institutes of Health R01 NS055099 and K24NS060951

Required Author Forms Disclosure forms provided by the authors are available with the online version of this article.

References

1. Rutkove SB, Aaron R, Shiffman CA. Localized bioimpedance analysis in the evaluation of neuromuscular disease. Muscle Nerve 2002;25:390–397.
2. Shiffman CA, Aaron R, Rutkove SB. Electrical impedance of muscle during isometric contraction. Physiol Meas 2003;24:213–234.
3. Tarulli AW, Duggal N, Esper GJ, et al. Electrical impedance myography in the assessment of disuse atrophy. Arch Phys Med Rehabil 2009;90:1806–1810.
4. Rutkove SB, Caress JB, Cartwright MS, et al. Electrical impedance myography as a biomarker to assess ALS progression. Amyotroph Lateral Scler 2012;13:439–445.
5. Zaidman CM, Wang LL, Connolly AM, et al. Electrical impedance myography in Duchenne muscular dystrophy and healthy controls: a multicenter study of reliability and validity. Muscle Nerve 2015;52:592–597.
6. Ahad MA, Fogerson PM, Rosen GD, Narayanswami P, Rutkove SB, Narayanaswami P. Electrical characteristics of rat skeletal muscle in immaturity, adulthood, and after sciatic nerve injury and their relation to muscle fiber size. Physiol Meas 2009;30:1415–1427.
7. Li J, Staats WL, Spieker A, Sung M, Rutkove SB. A technique for performing electrical impedance myography in the mouse hind limb: data in normal and ALS SOD1 G93A animals. PLOS ONE 2012;7:e45004.
8. Li J, Geisbush TR, Rosen GD, Lachey J, Mulivor A, Rutkove SB. Electrical impedance myography for the in vivo and ex vivo assessment of muscular dystrophy (mdx) mouse muscle. Muscle Nerve 2014;49:829–835.
9. Li J, Geisbush TR, Arnold WD, Rosen GD, Zaworski PG, Rutkove SB. A comparison of three electrophysiological methods for the assessment of disease status in a mild spinal muscular atrophy mouse model. PLOS ONE 2014;9:e111428.
10. Jafarpoor M, Li J, White JK, Rutkove SB. Optimizing electrode configuration for electrical impedance measurements of muscle via the finite element method. IEEE Trans Biomed Eng 2013;60:1446–1452.
11. Eisenberg RS. The equivalent circuit of single crab muscle fibers as determined by impedance measurements with intracellular electrodes. J Gen Physiol 1967;50:1785–1806.
12. Mobley BA, Leung J, Eisenberg RS. Longitudinal impedance of skinned frog muscle fibers. J Gen Physiol 1974;63:625–637.
13. Mobley B, Eidt G. Transverse impedance of single frog skeletal muscle fibers. Biophys J 1982;40:51–59.
14. Fatt P. An analysis of the transverse electrical impedance of striated muscle. Proc R Soc Lond B Biol Sci 1964;159:606–651.
15. Epstein BR, Foster KR. Anisotropy in the dielectric properties of skeletal muscle. Med Biol Eng Comput 1983;21:51–55.
16. Wang Y, Schimpf PH, Haynor DR, Kim Y. Geometric effects on resistivity measurements with four-electrode probes in isotropic and anisotropic tissues. IEEE Trans Biomed Eng 1998;45:877–884.
17. Kubicek WG, Karnegis JN, Patterson RP, Witsoe DA, Mattson RH. Development and evaluation of an impedance cardiac output system. Aerosp Med 1966;37:1208–1212.
18. Kubicek WG, Patterson RP, Witsoe DA. Impedance cardiogaphy as a noninvasive method for monitoring cardiac function and other parameters of the cardiovascular system. Ann N Y Acad Sci 1970;170:724–732.
19. Hoffer EC, Meador CK, Simpson DC. Correlation of whole-body impedance with total body water volume. J Appl Physiol 1969;27:531–534.
20. Lukaski HC, Johnson PE, Bolonchuk WW, Lykken GI. Assessment of fat-free mass using bioelectrical impedance measurements of the human body. Am J Clin Nutr 1985;41:810–817.
21. Aberg P, Nicander I, Hansson J, Geladi P, Holmgren U, Ollmar S. Skin cancer identification using multifrequency electrical impedance—a potential screening tool. IEEE Trans Biomed Eng 2004;51:2097–2102.
22. Stojadinovic A, Nissan A, Gallimidi Z, et al. Electrical impedance scanning for the early detection of breast cancer in young women: preliminary results of a multicenter prospective clinical trial. J Clin Oncol 2005;23:2703–2715.
23. Brown BH. Electrical impedance tomography (EIT): a review. J Med Eng Technol 2009;27:97–108.
24. Schwan HP. Alternating current electrode polarization. Biophysik 1966;3:181–201.
25. Schwan HP. Electrode polarization impedance and measurements in biological materials. Ann N Y Acad Sci 1968;148:191–209.
26. Searle A, Kirkup L. A direct comparison of wet, dry and insulating bioelectric recording electrodes. Physiol Meas 2000;21:271–283.
27. Chi YM, Tzyy-Ping Jung T-P, Cauwenberghs G. Dry-contact and noncontact biopotential electrodes: methodological review. IEEE Rev Biomed Eng 2010;3:106–119.

28. Meziane N, Webster JG, Attari M, Nimunkar AJ. Dry electrodes for electrocardiography. Physiol Meas 2013;34:R47–R69.
29. Lewes D. Electrode jelly in electrocardiography. Br Heart J 1965;27:105–115.
30. Geddes LA, Valentinuzzi ME. Temporal changes in electrode impedance while recording the electrocardiogram with "dry" electrodes. Ann Biomed Eng 1973;1:356–367.
31. Catrysse M, Puers R, Hertleer C, Van Langenhove L, van Egmond H, Matthys D. Towards the integration of textile sensors in a wireless monitoring suit. Sensors Actuators A Phys 2004;114:302–311.
32. Li Z, Li Y, Liu M, Cui L, Yu Y. Microneedle electrode array for electrical impedance myography to characterize neurogenic myopathy. Ann Biomed Eng 2016;44:1566–1575.
33. Rutkove SB, Partida RA, Esper GJ, Aaron R, Shiffman CA. Electrode position and size in electrical impedance myography. Clin Neurophysiol 2005;116:290–299.
34. Sanchez B, Pacheck A, Rutkove SB. Guidelines to electrode positioning for human and animal electrical impedance myography research. Sci Rep 2016;6:32615.
35. Geselowitz DB. An application of electrocardiographic lead theory to impedance plethysmography. IEEE Trans Biomed Eng 1971;18:38–41.
36. Cole KS, Baker RF. Longitudinal impedance of the squid giant axon. J Gen Physiol 1941;24:771–788.
37. Schwan HP, Sittel K. Wheatstone bridge for admittance determinations of highly conducting materials at low frequencies. Trans Am Inst Electr Eng Part I Commun Electron 1953;72:114–121.
38. Jones G, Josephs RC. The measurement of the conductance of electrolytes. I. An experimental and theoretical study of principles of design of the Wheatstone bridge for use with alternating currents and an improved form of direct reading alternating current bridge. J Am Chem Soc 1928;50:1049-1092.
39. Li N, Xu H, Wang W, Zhou Z, Qiao G, Li DD-U. A high-speed bioelectrical impedance spectroscopy system based on the digital auto-balancing bridge method. Meas Sci Technol 2013;24:65701.
40. Ackmann JJ. Complex bioelectric impedance measurement system for the frequency range from 5 Hz to 1 MHz. Ann Biomed Eng 1993;21:135–146.
41. Masciotti JM, Lasker JM, Hielscher AH. Digital lock-in detection for discriminating multiple modulation frequencies with high accuracy and computational efficiency. IEEE Trans Instrum Meas 2008;57:182–189.
42. Shiffman CA. Adverse effects of near current-electrode placement in non-invasive bio-impedance measurements. Physiol Meas 2013;34:1513–1529.
43. Bao JZ, Davis CC, Schmukler RE. Impedance spectroscopy of human erythrocytes: system calibration and nonlinear modeling. IEEE Trans Biomed Eng 1993;40:364–378.
44. Sanchez B, Schoukens J, Bragos R, Vandersteen G. Novel Estimation of the electrical bioimpedance using the local polynomial method. application to in-vivo real-time myocardium tissue impedance characterization during the cardiac cycle. IEEE Trans Biomed Eng 2011;58:2–4.
45. Sanchez B, Louarroudi E, Jorge E, Cinca J, Bragos R, Pintelon R. A new measuring and identification approach for time-varying bioimpedance using multisine electrical impedance spectroscopy. Physiol Meas 2013;34:339–357.
46. Sanchez B, Louarroudi E, Bragos R, Pintelon R. Harmonic impedance spectra identification from time-varying bioimpedance: theory and validation. Physiol Meas 2013;34:1217–1238.
47. Sanchez B, Louarroudi E, Pintelon R. Time-invariant measurement of time-varying bioimpedance using vector impedance analysis. Physiol Meas 2015;36:595–620.
48. Sanchez B, Fernandez X, Reig S, Bragos R. An FPGA-based frequency response analyzer for multisine and stepped sine measurements on stationary and time-varying impedance. Meas Sci Technol 2014;25:15501.
49. al-Hatib F. Patient-instrument connection errors in bioelectrical impedance measurement. Physiol Meas 1998;19:285–296.
50. Bolton MP, Ward LC, Khan A, et al. Sources of error in bioimpedance spectroscopy. Physiol Meas 1998;235:235-245.
51. Scharfetter H, Hartinger P, Hinghofer-Szalkay H, Hutten H. A model of artefacts produced by stray capacitance during whole body or segmental bioimpedance spectroscopy. Physiol Meas 1998;19:247–261.
52. Buendia R, Seoane F, Bosaeus I, et al. Robustness study of the different immittance spectra and frequency ranges in bioimpedance spectroscopy analysis for assessment of total body composition. Physiol Meas 2014;35:1373–1395.
53. Sanchez B, Aroul AP, Bartolome E, Soundarapandian K, Bragos R. Propagation of measurement errors through body composition equations for body impedance analysis. IEEE Trans Instrum Meas 2014;63:1535–1544.
54. Bogónez-Franco P, Nescolarde L, Bragos R, Rosell-Ferrer J, Yandiola I. Measurement errors in multifrequency bioelectrical impedance analyzers with and without impedance electrode mismatch. Physiol Meas 2009;30:573–587.
55. Lozano A, Rosell J, Pallás-Areny R. Errors in prolonged electrical impedance measurements due to electrode repositioning and postural changes. Physiol Meas 1995;16:121–130.
56. Cornish BH, Eles PT, Thomas BJ, Ward LC. The effect of electrode placement in measuring ipsilateral/contralateral segmental bioelectrical impedance. Ann N Y Acad Sci 2000;904:221–224.
57. Moon JR, Stout JR, Smith AE, et al. Reproducibility and validity of bioimpedance spectroscopy for tracking changes in total body water: implications for repeated measurements. Br J Nutr 2010;104:1384–1394.
58. Grisbrook TL, Kenworthy P, Phillips M, Gittings PM, Wood FM, Edgar DW. Alternate electrode placement for whole body and segmental bioimpedance spectroscopy. Physiol Meas 2015;36:2189–2201.
59. Ayllón D, Gil-Pita R, Seoane F. Detection and classification of measurement errors in bioimpedance spectroscopy. PLOS ONE 2016;11:e0156522.
60. Levenberg K. A method for the solution of certain non-linear problems in least squares. Q J Appl Math 1944;2:164–168.
61. Marquardt DW. An algorithm for least-squares estimation of nonlinear parameters. J Soc Ind Appl Math 1963;11:431–441.
62. Cole KS. Permeability and impermeability of cell membranes for ions. Cold Spring Harb Symp Quant Biol 1940;8:110–122.
63. Foster KR, Schwan HP. Dielectric properties of tissues and biological materials: a critical review. Crit Rev Biomed Eng 1989;17:25–104.
64. Rush S, Abildskov JA, McFee R. Resistivity of body tissues at low frequencies. Circ Res 1963;12:40–50.
65. Zheng E, Shao S, Webster JG. Impedance of skeletal muscle from 1 Hz to 1 MHz. IEEE Trans Biomed Eng 1984;BME-31:477–481.
66. Rush S. Methods of measuring the resistivities of anisotropic conducting media. J Res 1962;66C:217–222.
67. Garmirian LP, Chin AB, Rutkove SB. Discriminating neurogenic from myopathic disease via measurement of muscle anisotropy. Muscle Nerve 2009;39:16–24.
68. Li J, Jafarpoor M, Bouxsein M, Rutkove SB. Distinguishing neuromuscular disorders based on the passive electrical material properties of muscle. Muscle Nerve 2015;51:49-55.
69. Tarulli A, Esper GJ, Lee KS, Aaron R, Shiffman CA, Rutkove SB. Electrical impedance myography in the bedside assessment of inflammatory myopathy. Neurology 2005;65:451–452.
70. Rutkove SB, Lee KS, Shiffman CA, Aaron R. Test-retest reproducibility of 50 kHz linear-electrical impedance myography. Clin Neurophysiol 2006;117:1244–1248.

71. Kortman HG, Wilder SC, Geisbush TR, Narayanaswami P, Rutkove SB. Age- and gender-associated differences in electrical impedance values of skeletal muscle. Physiol Meas 2013;34: 1611–1622.
72. Sung M, Li J, Spieker AJ, et al. Spaceflight and hind limb unloading induce similar changes in electrical impedance characteristics of mouse gastrocnemius muscle. J Musculoskelet Neuronal Interact 2013;13:405–411.
73. Li J, Spieker AJ, Rosen GD, Rutkove SB. Electrical impedance alterations in the rat hind limb with unloading. J Musculoskelet Neuronal Interact 2013;13:37–44.
74. Wang LL, Spieker AJ, Li J, Rutkove SB. Electrical impedance myography for monitoring motor neuron loss in the SOD1 G93A amyotrophic lateral sclerosis rat. Clin Neurophysiol 2011;122:2505–2511.
75. Rutkove SB, Shefner JM, Gregas M, et al. Characterizing spinal muscular atrophy with electrical impedance myography. Muscle Nerve 2010;42:915–921.
76. Rutkove SB, Gregas MC, Darras BT. Electrical impedance myography in spinal muscular atrophy: a longitudinal study. Muscle Nerve2012;45:642–647.
77. Chin AB, Garmirian LP, Nie R, Rutkove SB. Optimizing measurement of the electrical anisotropy of muscle. Muscle Nerve 2008;37:560–565.
78. Li J, Pacheck A, Sanchez B, Rutkove SB. Single and modeled multifrequency electrical impedance myography parameters and their relationship to force production in the ALS SOD1G93A mouse. Amyotroph Lateral Scler Frontotemporal Degener 2016;1–7.
79. Rutkove SB, Zhang H, Schoenfeld DA, et al. Electrical impedance myography to assess outcome in amyotrophic lateral sclerosis clinical trials. Clin Neurophysiol 2007;118:2413–2418.
80. Shellikeri S, Yunusova Y, Green JR, et al. Electrical impedance myography in the evaluation of the tongue musculature in amyotrophic lateral sclerosis. Muscle Nerve 2015;52:584-591.
81. McIlduff, CE, Yim S, Pacheck A, Geisbush T, Mijailovic A RS. An improved electrical impedance myography tongue array for use in clinical trials. Clin Neurophysiol 2016;127:932-935.
82. Pacheck A, Mijailovic A, Yim S, et al. Tongue electrical impedance in amyotrophic lateral sclerosis modeled using the finite element method. Clin Neurophysiol 2016;127:1886-1890.
83. Li J, Sung M, Rutkove SB. Electrophysiologic biomarkers for assessing disease progression and the effect of riluzole in SOD1 G93A ALS mice. PLOS ONE 2013;8:e65976.
84. Ahad MA, Narayanaswami P, Kasselman LJ, Rutkove SB. The effect of subacute denervation on the electrical anisotropy of skeletal muscle: implications for clinical diagnostic testing. Clin Neurophysiol 2010;121:882–886.
85. Kolb SJ, Coffey CS, Yankey JW, et al. Baseline results of the NeuroNEXT spinal muscular atrophy infant biomarker study. Ann Clin Transl Neurol 2016;3:132–145.
86. Arnold WD, McGovern VL, Sanchez B, et al. The neuromuscular impact of symptomatic SMN restoration in a mouse model of spinal muscular atrophy. Neurobiol Dis 2016;87:116–123.
87. Rutkove SB, Esper GJ, Lee KS, Aaron R, Shiffman CA. Electrical impedance myography in the detection of radiculopathy. Muscle Nerve 2005;32:335–341.
88. Spieker AJ, Narayanaswami P, Fleming L, Keel JC, Muzin SC, Rutkove SB. Electrical impedance myography in the diagnosis of radiculopathy. Muscle Nerve 2013;48:800–805.
89. Banker B, Engel A. Basic reactions of muscle. In: Engel A, Franzini-Armstrong C, editors. Myology. 3rd ed. New York: McGraw-Hill; 2004. pp. 691–748.
90. Brooke MH, Engel WK. The histographic analysis of human muscle biopsies with regard to fiber types. 4. Children's biopsies. Neurology 1969;19:591–605.
91. Rutkove SB, Geisbush TR, Mijailovic A, et al. Cross-sectional evaluation of electrical impedance myography and quantitative ultrasound for the assessment of duchenne muscular dystrophy in a clinical trial setting. Pediatr Neurol 2014;51:88–92.
92. Wu JS, Li J, Greenman RL, Bennett D, Geisbush T, Rutkove SB. Assessment of aged mdx mice by electrical impedance myography and magnetic resonance imaging. Muscle Nerve 2015;52:598–604.
93. Sanchez B, Li J, Yim S, Pacheck A, Widrick JJ, Rutkove SB. Evaluation of electrical impedance as a biomarker of myostatin inhibition in wild type and muscular dystrophy mice. PLOS ONE 2015;10:e0140521.
94. Statland JM, Heatwole C, Eichinger K, Dilek N, Martens WB, Tawil R. Electrical impedance myography in facioscapulohumeral muscular dystrophy. Muscle Nerve 2016;54:696-701.
95. Urso ML, Clarkson PM, Price TB (2006) Immobilization effects in young and older adults. Eur J Appl Physiol 96:564–571.
96. Esper GJ, Lee KS, Shiffman CA, Aaron R, Bradonjic K, Rutkove SB. Electrical impedance myography in the assessment of age-associated muscle change. 52nd Annu. Sci. Meet. Am. Assoc. Neuromuscul. Electrodiagn. Med. Monterey, CA, USA; 2005.
97. Iannuzzi-Sucich M, Prestwood KM, Kenny AM. Prevalence of sarcopenia and predictors of skeletal muscle mass in healthy, older men and women. J Gerontol A Biol Sci Med Sci 2002;57:M772-M777.
98. Janssen I, Heymsfield SB, Wang ZM, Ross R. Skeletal muscle mass and distribution in 468 men and women aged 18-88 yr. J Appl Physiol 2000;89:81–88.
99. Nescolarde L, Yanguas J, Lukaski H, Alomar X, Rosell-Ferrer J, Rodas G. Localized bioimpedance to assess muscle injury. Physiol Meas 2013;34:237–245.
100. Nescolarde L, Yanguas J, Lukaski H, Alomar X, Rosell-Ferrer J, Rodas G. Effects of muscle injury severity on localized bioimpedance measurements. Physiol Meas 2015;36:27–42.
101. Biogen. Methodology study of novel outcome measures to assess progression of ALS. NCT02611674. Available at: https://clinicaltrials.gov/ct2/show/NCT02611674.
102. Sanchez B, Li J, Bragos R, Rutkove SB. Differentiation of the intracellular structure of slow- versus fast-twitch muscle fibers through evaluation of the dielectric properties of tissue. Phys Med Biol 2014;59:1–12.
103. McClendon JF. The increased permeability of striated muscle to ions during contraction. Am J Physiol Leg Content 1912;29:302–305.
104. Dubuisson M. Recherches sur les modifications qui survien-nent dans la conductibilité électrique du muscle au cours de la contraction. Arch Int Physiol 1933;37:35–57.
105. Bozler E. The change of alternating current impedance of muscle produced by contraction. J Cell Comp Physiol 1935;6:217–228.
106. Bozler E, Cole KS. Electric impedance and phase angle of muscle in rigor. J Cell Comp Physiol 1935;6:229–241.
107. Rutkove SB. Electrical impedance myography: background, current state, and future directions. Muscle Nerve 2009;40:936–946.
108. Zagar T, Krizaj D. Multivariate analysis of electrical impedance spectra for relaxed and contracted skeletal muscle. Physiol Meas 2008;29:S365-S372.
109. Silva OL, Hoffman IO, Aya JC, et al. In vivo measurement of skeletal muscle impedance from rest to fatigue. Technol Med Sci 2011. doi:10.1201/b11330-27.
110. Sanchez B, Li J, Geisbush T, Bragos R, Rutkove S. Impedance alterations in healthy and diseased mice during electrically-induced muscle contraction. IEEE Trans Biomed Eng 2016;63: 1602–1612.
111. Frerichs I. Electrical impedance tomography (EIT) in applications related to lung and ventilation: a review of experimental and clinical activities. Physiol Meas 2000;21:R1-R21.

112. Halter RJ, Hartov A, Paulsen KD. A broadband high-frequency electrical impedance tomography system for breast imaging. IEEE Trans Biomed Eng 2008;55:650–659.
113. Wan Y, Borsic A, Heaney J, et al. Transrectal electrical impedance tomography of the prostate: spatially coregistered pathological findings for prostate cancer detection. Med Phys 2013;40:63102.
114. Fabrizi L, McEwan A, Oh T, Woo EJ, Holder DS. An electrode addressing protocol for imaging brain function with electrical impedance tomography using a 16-channel semi-parallel system. Physiol Meas 2009;30:S85-S101.
115. Silva OL. Muscle contraction dectection using electrical impedance tomography. Escola Politecnica da Universidade de Sao Paulo; 2012.
116. Silva OL, Sousa THS, Hoffman IO, et al. A proposal to monitor muscle contraction through the change of electrical impedance inside a muscle. 5th IEEE RAS/EMBS Int. Conf. Biomed. Robot. Biomechatronics. IEEE; 2014. p. 763–767.
117. Rodriguez S, Ollmar S, Member S, Waqar M, Member S. A batteryless sensor ASIC for implantable bio-impedance applications. IEEE Trans Biomed Circuits Syst 2016;10:533-544.